

# Effect of chemical composition on sintering and properties of $\text{Al}_2\text{O}_3$ – $\text{SiO}_2$ system derived from sillimanite beach sand

H.S. Tripathi\*, G. Banerjee

*Central Glass & Ceramic Research Institute, Refractories Division, Calcutta 700 032, India*

Received 2 June 1997; accepted 2 September 1997

## Abstract

Reaction sintering of beach sand sillimanite and alumina is an innovative as well as inexpensive method of mullite formation. Beach sand sillimanite, a by-product generated during the separation of rare earth compounds, and calcined alumina were used as starting materials and were mixed in appropriate proportion and sintered in compacted form at 1500–1575°C. The study reveals that the use of submicron size powder enhances the sintering process. In this investigation, effect of chemical composition on sintering and mechanical/thermomechanical properties has been studied. It was found that the densification process is dependent on the  $\text{Al}_2\text{O}_3/\text{SiO}_2$  ratio. Silica rich composition achieves highest density at 1525°C whereas the alumina rich composition requires 1550°C. Flexural strength measured at room temperature and at 1200°C initially decreases with alumina content, with a minima at 71–74%  $\text{Al}_2\text{O}_3$  and then increases again. Microstructure of the sintered is also dependent on the  $\text{Al}_2\text{O}_3/\text{SiO}_2$  ratio of the batch. Mullite made from silica rich composition is needle shape in nature whereas in alumina rich composition they are non-acicular in nature. © 1998 Elsevier Science Limited and Techna S.r.l. All rights reserved

## 1. Introduction

Efforts have been made earlier to develop mullite ceramics by reaction sintering [1–4].  $\text{Al}_2\text{O}_3$  containing reactants traditionally used for this purpose are alumina, refractory grade bauxite, clay and in few cases sillimanite group of minerals. A gradual depletion of these naturally occurring high alumina raw materials has made a serious challenge to the refractory industries to keep on continued production of such refractory, that is in high demand. In view of this it has become imperative to find alternate sources of high alumina aggregate. India is one of the few countries in the world that has significant deposits of beach sands. Beach sand sillimanite, a by-product generated in large amount during the separation of rare earth oxide, does not find wide application in refractory industries primarily due to its fineness. The successful use of this material is dependent on aggregate making.

Although a number of authors have studied the thermal transformation of sillimanite to mullite [5,6], the work on beach sand sillimanite is limited.

Sillimanite sand on heating decomposes to mullite and amorphous silica in the temperature range 1500–1650°C depending on the particle size and impurity level.



The product quality can be improved by combining the silica released during decomposition of sillimanite by the addition of alumina. The present investigation was carried out to develop mullite/mullite-corundum aggregate from beach sand sillimanite for its commercial utilisation. Thus the mullite/mullite-corundum aggregates were produced by a process of reaction sintering. In this investigation an attempt has been made to study the effect of chemical composition on the densification of  $\text{SiO}_2$ – $\text{Al}_2\text{O}_3$  system derived from beach sand sillimanite and alumina. Attempt has also been made to study the compositional effect on the mechanical/thermomechanical properties and microstructure of the aggregate developed.

## 2. Experimental

Beach sand sillimanite obtained from Indian Rare Earths Limited (IREL), India and commercial calcined

\* Corresponding author.

alumina obtained from Indian Aluminium Company Ltd. (INDAL), India, were used in this investigation. The particle size distribution of the starting sillimanite powder and calcined alumina were determined in a sedigraph apparatus using calgon as dispersing agent.

The chemical analyses were done by a conventional wet chemical method. Five batch compositions were studied namely S, M, Cl, C2 & C3 having 57.6, 70.54, 73.42, 76.29 and 79.16 wt% alumina, respectively. To enhance the reaction sintering all the batches were attrition-milled in a water medium in a zirconia pot using zirconia ball. The surface area of the milled powder was determined by BET method in a BET apparatus (Sorpty 1750, Carlo Erba, Italy). Surface area of the powders was determined at regular intervals. The optimum milling time is selected by studying the surface area against milling time. The slurries thus obtained were dried at 1105°C, crushed to break the agglomerates, mixed with organic binder and uniaxially pressed at a pressure of 120 MPa. After drying at  $110 \pm 5^\circ\text{C}$  these samples were fired at a temperature varying from 1500 to 1575°C at an interval of 25°C with a 2 h soaking period. Firing was done in an electric furnace and the heating rate was  $5^\circ\text{C min}^{-1}$  up to 1100°C, after that  $3^\circ\text{C min}^{-1}$  up to the final firing temperature. Fired products thus obtained were characterised in terms of linear shrinkage, bulk density, apparent porosity, flexural strength, at room temperature (RT) as well as at 1200°C. Phase identification and microstructural analysis were done by X-ray diffraction study (XRD) and scanning electron microscopy (SEM) and infrared spectroscopy (IR).

Bulk density and apparent porosity of the sintered product were measured by a conventional method using Archimedes' principle in water medium.

Flexural strength at room temperature was determined by the three point bending method in an apparatus (Instron) with a span length of 40 mm and crosshead speed of  $0.5 \text{ mm min}^{-1}$  for a test bar of  $6 \times 6 \times 50 \text{ mm}^3$ . The samples used were polished and

edges were chamfered with a diamond disc. Hot MOR was also determined by the three point bending method at 1200°C.

X-ray diffraction pattern of the raw materials and sintered product were obtained in a diffractometer using Ni-filter and  $\text{Cu-K}_\alpha$  radiation. Diffraction patterns were recorded in the Braggs angle ( $2\theta$ ) range  $15\text{--}60^\circ$ . Micro-structure of the sintered product was investigated using sputtered gold coating on the polished surface after chemical (HF) and thermal etching. IR-spectrometer was used to record IR transmission spectra using KBr disc method, and IR transmission was recorded over the wave number range 400 to  $4000 \text{ cm}^{-1}$ .

### 3. Results and Discussion

#### 3.1. Raw material characterisation

The chemical analyses of the raw materials used in this investigation are given in Table 1. Microscopic observation under polarising microscope and XRD study reveal that the mineral present in the sillimanite beach sand is mostly sillimanite associated with small amounts of quartz and kaolinite as impurities. Table 1 shows that  $\text{SiO}_2$  content of the sillimanite sand (40.3%) is higher than the stoichiometric amount. This excess  $\text{SiO}_2$  occurs in the sand as quartz which is confirmed from XRD pattern (Fig. 1). The IR pattern of the sillimanite sand is shown in Fig. 2. The absorption peak at  $1175 \text{ cm}^{-1}$  also clearly indicates that this mineral is sillimanite.

Particle size distribution of the starting sillimanite powder (obtained by vibromilling) and as received commercial alumina used in this study are shown in Fig. 3. The average particle size of the sillimanite and

Table 1  
Chemical composition of the raw materials

Component	Wt%	
	Sillimanite	Alumina
$\text{Al}_2\text{O}_3$	57.6	99.3
$\text{SiO}_2$	40.3	—
$\text{Fe}_2\text{O}_3$	0.31	
$\text{TiO}_2$	0.11	
$\text{CaO}$	0.42	
$\text{MgO}$	0.31	
$\text{Na}_2\text{O}$	—	0.30
$\text{K}_2\text{O}$	0.02	
LOI	0.70	0.02
Phase analysis	Major-sillimanite Minor-quartz, kaolinite	$\alpha$ -alumina

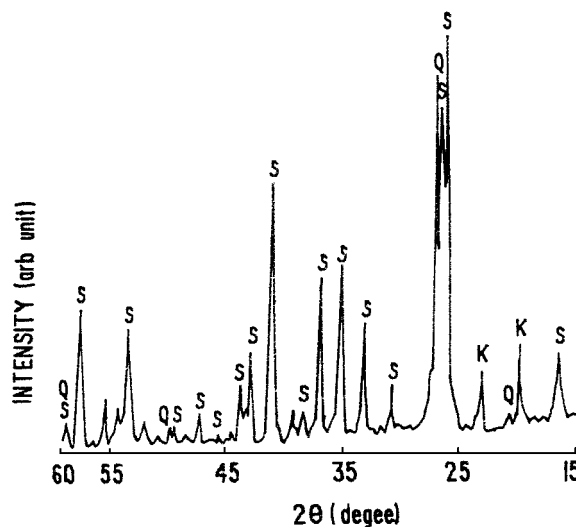


Fig. 1. X-ray diffraction pattern of beach sand sillimanite. S—sillimanite, Q—quartz, K—kaolinite.

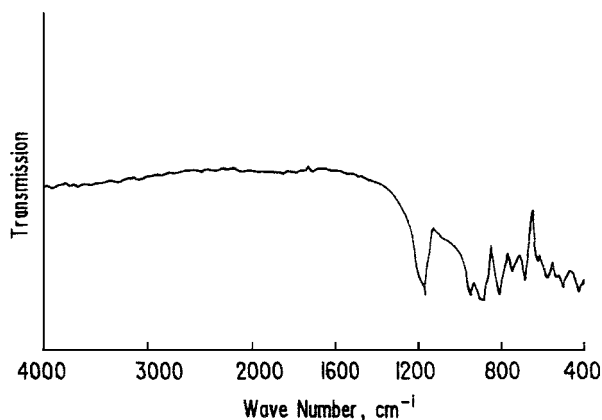


Fig. 2. Infrared transmission spectrum of sillimanite sand.

alumina are 4.5 and 5.0  $\mu\text{m}$ , respectively. Five different batches are selected for this investigation and their composition and sample code are given in Table 2.

All the batches are attrition milled for a definite time period, obtained by studying the variation of specific surface area against milling time. As shown in Fig. 4, the specific surface area increases with milling time up to 9 h and beyond that, although it increases with time, the variation is not appreciable. Hence a optimum milling time of 9 h is chosen for all the batches used in this investigation. Since all the batches are attrition milled for a specific time of 9 h; they have similar particle size distribution which is reflected in the apparent porosity data of the green compact after uniaxial pressing. They are in a close range of 44.2–45%.

### 3.2. Effect of chemical composition on densification

Investigation on the aggregate developed revealed that silica rich mullite aggregate (S) has undergone

Table 2  
Batch Composition

Sample Code	Sillimanite	Alumina	Al <sub>2</sub> O <sub>3</sub> content in the batch (wt%)
S	200	nil	57.60
M	140	63.00	70.54
C1	125	76.39	73.42
C2	115	93.44	16.29
C3	100	107.10	79.16

appreciable shrinkage when fired at 1525°C, whereas it is 1550°C for the other composition, as shown in Fig. 5. It was found that the ultimate linear shrinkage at 1575°C is almost the same (16.16–16.39 %) in all the cases irrespective of alumina content. The rate of densification of silica rich composition was relatively high compared to the other composition. The bulk density of the aggregates were directly proportional to alumina content and this trend was observed at all firing temperatures. Fig. 6 indicates that densification behavior is dependent on the alumina content. [7,8] Silica rich composition (S) achieves its highest bulk density at 1525°C. The highest B. D. of mullite composition (M) achieved at 1550°C has the value of 3.16, which is close to the true density of the mullite. Since the sillimanite beach sand contains several impurities, the densification proceeds through liquid phase sintering. It was found that bulk density increases with firing temperature up to a certain level irrespective of the Al<sub>2</sub>O<sub>3</sub> content. Beyond this temperature it decreases due to the excessive formation of vitreous phase and closed pores. Apparent porosity data also supports the above observation.

The XRD pattern of sillimanite and mullite is very close, and it is very difficult to measure mullite content of the batches quantitatively by this method. However, infrared technique may be used to distinguish sillimanite

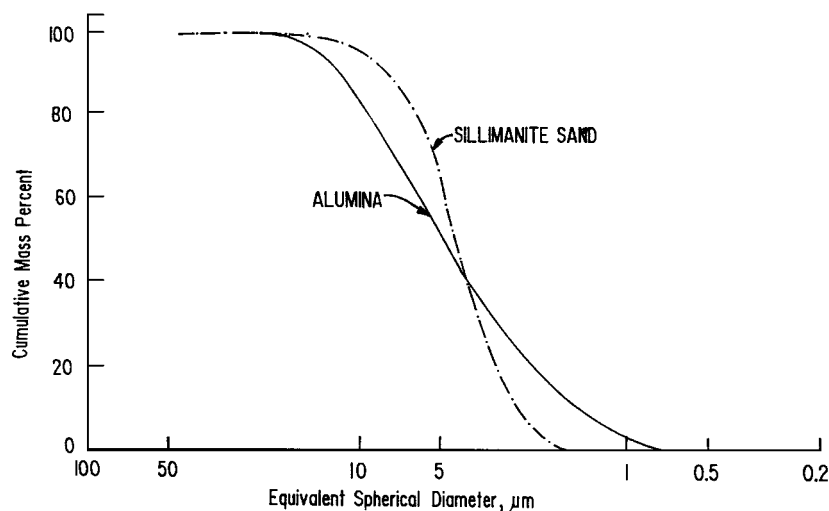


Fig. 3. Particle size distribution of the starting raw materials.

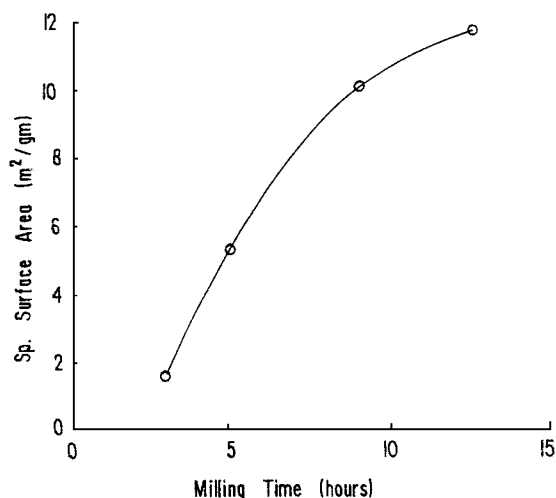


Fig. 4. Effect of milling time on the specific surface area of the batch.

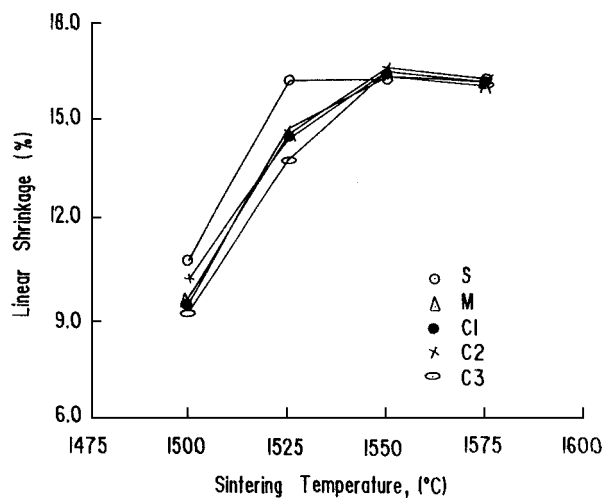


Fig. 5. Variation of linear shrinkage with sintering temperature.

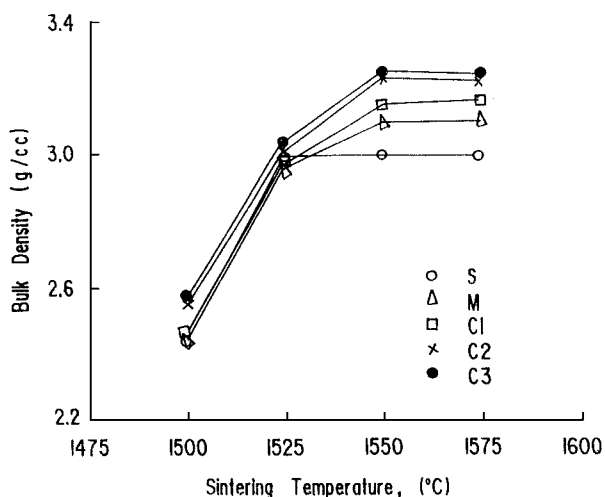


Fig. 6. Effect of sintering temperature on the bulk density of the samples.

and mullite in the fired product [9,10]. Even Roy et al. [11] show that it is possible to determine quantitatively the unreacted sillimanite in the sintered product. IR pattern of the sintered body is shown in Fig. 7. The total absence of the characteristic sillimanite absorption peak at  $1175\text{ cm}^{-1}$  in all the compositions fired at  $1525^\circ\text{C}$  clearly indicates complete conversion of sillimanite to mullite at this temperature. Hence XRD together with IR technique are used to identify the crystalline phases in the fired product.

### 3.3. Microstructure

All the samples except S achieve their highest bulk density at a firing temperature of  $1550^\circ\text{C}$ . Microstructural evaluation were done on these samples. Scanning electron photomicrograph of the samples S, M, C1, C2, C3 fired at  $1550^\circ\text{C}/2\text{ h}$  are shown in Fig. 8. In S sample the mullite crystals with orthorhombic habit of sillimanite was found. The black voids in the micrograph are due to the dissolution of the silicate phase in HF during chemical leaching as shown in Fig. 8(a). Addition of  $\text{Al}_2\text{O}_3$  into the batch reduces the silicate phase as a result of mullite formation. The resulting microstructures are in compact form with a higher degree of grain to grain interlocking as shown in Fig. 8(b)–(e). In all the cases mullite crystals retains the crystalline habit of sillimanite, some non-acicular or pallets of mullite were found in the alumina rich sample C2 and C3. Some earlier workers also reported such findings [12]. Intergranular Vitreous phase is less in C1 composition and higher on either side of this. Table 4 also supported the same result. In samples C2 and C3 the hexagonal crystals of corundum were evenly distributed within the mullite matrix.

### 3.4. Strength

Flexural strength at room temperature of the aggregates as a function of alumina content and sintering

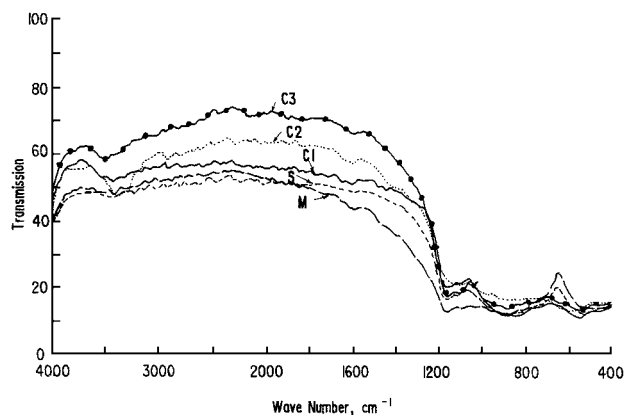


Fig. 7. IR pattern of the samples sintered at  $1525^\circ\text{C}/2\text{ h}$ .

temperature are shown in Fig. 9. Each aggregate develops highest room temperature flexural strength at 1550°C. Strength of silica rich aggregate (S) was maximum at all temperatures and a maximum strength of 161 MPa was observed for “S” composition fired at 1550°C. At all firing temperatures the curves show a

minima around mullite composition “M”, and it is higher on either side of this. Thus the flexural strength at room temperature is very much dependent on the  $\text{Al}_2\text{O}_3/\text{SiO}_2$  ratio.

High temperature flexural strength (at 1200°C) was also found to be dependent on the  $\text{Al}_2\text{O}_3/\text{SiO}_2$  ratio and

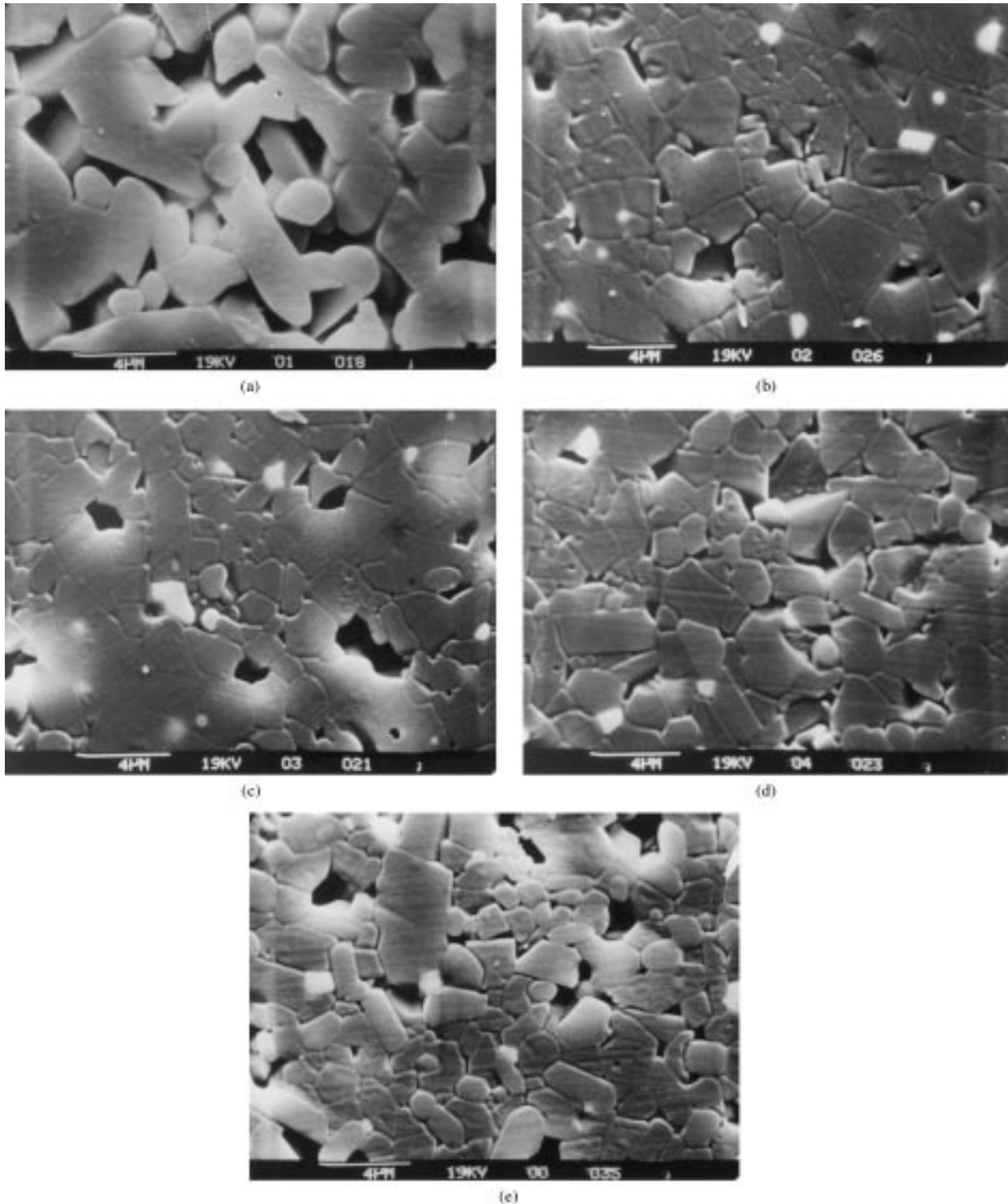


Fig. 8. Scanning electron micrographs of the samples sintered at 1550°C: (a) sample S, (b) sample M, (c) sample C1, (d) sample C2, (e) sample C3.

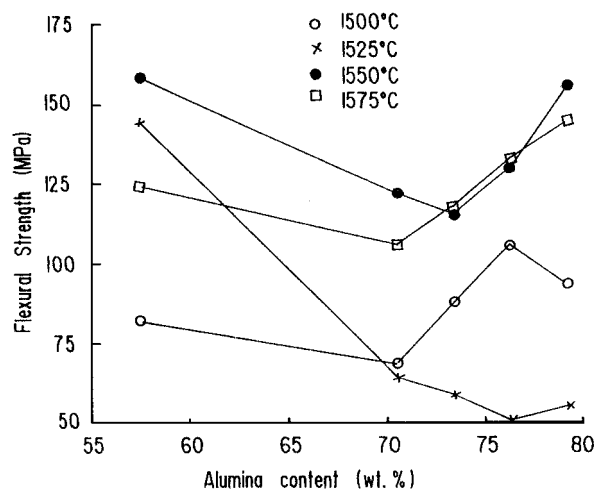


Fig. 9. Variation of room temperature flexural strength with chemical composition of the samples sintered at different temperatures.

firing temperature (Fig. 10). At all sintering temperature the flexural strength at 1200°C of silica rich composition (S) was maximum. At high temperature, softening of the glassy phase occurs, which is responsible for stress relaxation at the crack tips, consequently increasing the HMOR [13]. The highest hot strength of 316 MPa was observed for “S” composition when fired at 1525°C. But in “C” composition that allows sufficient corundum grains in the sintered body shows an increasing tendency in the hot strength at a sintering temperature of 1575°C. Fig. 10 shows that the high temperature flexural strength at 1200°C initially decreases with  $\text{Al}_2\text{O}_3$  content where there was lower amount of glassy phase and then again increases with  $\text{Al}_2\text{O}_3$  content.

Glassy phase present in the sintered product (1575°C) was estimated by HF leaching technique [14], the results indicate (Table 3) that the glassy phase is also dependent on the composition. It is minimum “C1” composition

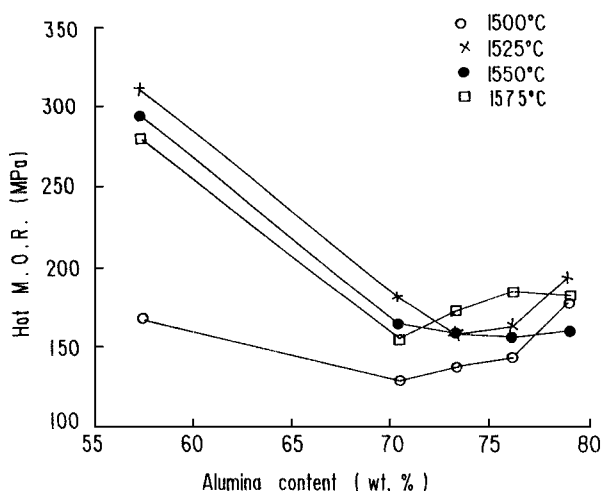


Fig. 10. Effect of  $\text{Al}_2\text{O}_3$  content on the flexural strength at 1200°C of the samples sintered at different temperatures.

Table 3

Silicate phase content of the product sintered at 1575°C

Sample	$\text{Al}_2\text{O}_3$ content (wt%)	Silicate phase content (wt%)
S	57.60	21.64
M	70.54	12.51
C1	73.42	9.17
C2	76.29	11.98
C3	79.16	15.83

(73.42 %  $\text{Al}_2\text{O}_3$ ) and higher on either side of this composition. Higher percent of glass in “M” composition is probably due to the incomplete mullitisation of the silica released during thermal decomposition of sillimanite sand. The alkali content increases with the addition of alumina and this is responsible for increased glassy phase in case of alumina rich composition. High temperature flexural strength is related to this glassy phase content, although the variation is not too high in alumina rich composition.

#### 4. Conclusion

The reaction sintering of beach sand sillimanite and calcined alumina has shown encouraging results when microfine particles were used (specific surface area  $10.1 \text{ m}^2 \text{ gm}^{-1}$ ). Densification of the system and properties of the sintered products are dependent on the alumina/silica ratio. All the compositions achieve their highest bulk density at 1550°C. Silica rich composition in sintered form had relatively high cold and hot flexural strength at 1200°C compared to all other compositions. High temperature flexural strength at 1200°C of compositions containing alumina in the range 71–74 % are lower than those with other alumina contents on either side of this. Mullite formed from sillimanite sand retains the crystal habit of sillimanite during thermal transformation. Non-acicular or pallet mullite were observed in alumina rich composition. Mullite compositions develop a compact microstructure with interlocking orthorhombic mullite crystals.

#### Acknowledgements

The authors are thankful to the Director, Central Glass & Ceramic Research Institute, Calcutta, India for his kind permission to publish this paper. The authors are also thankful to S. K. Das, B. Mukherjee and A. Ghosh, Scientists of this Institute for their active support to carry out this work. The work has been carried out under a CSIR research fellowship for Ph.D.(Tech.) degree of the first author who is thankful to the CSIR for necessary funding.

## References

- [1] I.A. Aksay, D.M. Dabbs, M. Sarikaya, Mullite for structural, electronic and optical applications, *J. Am. Ceram. Soc.* 74 (1991) 2343–2358.
- [2] B. Saruhan, W. Albers, H. Schneider, W.A. Kaysser, Reaction sintering mechanism of mullite in the systems cristobalite/  $\alpha$ - $\text{Al}_2\text{O}_3$  and amorphous  $\text{SiO}_2$ / $\alpha$ - $\text{Al}_2\text{O}_3$ , *J. Eur. Ceram. Soc.* 16 (1996) 1075–1081.
- [3] Y. Nurishi, J.A. Pask, Sintering of  $\alpha$ - $\text{Al}_2\text{O}_3$ / amorphous silica compacts, *Ceram. Int.* 8 (1982) 57–59.
- [4] P.D.D. Rodrigo, P. Boch, High purity mullite ceramics by reaction sintering, *Int. J. High Tech. Ceram.* 1 (1985) 3–30.
- [5] H. Schneider, A. Majdic, Preliminary investigation on the kinetics of high temperature transformation of sillimanite to 3/2 mullite plus silica acid comparison with the behaviour of andalusite and kyanite, *Sci. Ceram.* 11 (1) 191–196.
- [6] H.H. Wilson, Mullite formation from sillimanite group of minerals, *Am. Ceram. Soc. Bull.* 48 (b) (1969) 796–797.
- [7] M.D. Sacks, J.A. Pask, Sintering of mullite containing materials: I Effect of chemical composition, *J. Am. Ceram. Soc.* 65 (21) (1982) 65–70.
- [8] G. Banerjee, H.S. Tripathi, K. Das, S.K. Das, Refractories—properties and applications, in: S. Kumar (Ed.), *Handbook of Ceramics*, Vol. II, Kumar and Associates, Calcutta, pp. 239–256.
- [9] R. Roy, E.E. Francis, On the distinction of sillimanite from mullite by infrared technique, *Amer. Miner.* 38 (1953) 725–28.
- [10] S.P. Chaudhury, The distinction between mullite and sillimanite: a review, *Interceram.* 3 (1981) 199–202.
- [11] A.S. Navale, N.K. Rao, S.P. Chakravorty, R. Raut, S.K. Roy, Analysis of minerals transformation by infrared spectroscopy: sillimanite to mullite., In *Proc. 5th National Symp. Analytical Spectroscopy including Hyphenated Technique*, Ind. Anal. Chemistry, M.D. Shastri, A.G. Page (Eds.), Bombay, 1988, pp. 115–119.
- [12] H. Schneider, K. Okada, J. Pask, *Mullite and Mullite Ceramics*, John Wiley & Sons, Chichester, UK, 1994.
- [13] S. Kanzaki, T. Kumazawa, J. Asami, O. Abe, H. Tabata, Dependency of mechanical property of sintered mullite on chemical composition, *Yogyo-Kyokai-Shi* 931 (71) (1985) 407–408.
- [14] Z. Wancheng, Z. Litong, F. Hengzhj, Modification of the hydrofluoric acid leaching technique: I, Corundum–mullite–glassy phase materials, *J. Am. Ceram. Soc.* 71 (5) (1988) 395–398.